Decomposition of skill scores for conditional verification – Impact of AMO phases on the predictability of decadal temperature forecasts

Andy Richling[1], Jens Grieger[1], and Henning W. Rust[1]

[1]Freie Universität Berlin, Institute of Meteorology, Carl-Heinrich-Becker Weg 6–10, 12165 Berlin, Germany

Correspondence: Andy Richling (andy.richling@fu-berlin.de)

Abstract. Since the performances of weather and climate forecasting systems and their competing reference systems are generally not homogeneous in time and space and may vary in specific situations, improvements in certain situations or subsets have different effects on overall skill. We present a decomposition of skill scores for the conditional verification of such systems. The aim is to evaluate the performance of a system individually for predefined subsets with respect to the overall performance. The overall skill score is decomposed into weighted sum representing *subset contributions*, where each individual contribution is the product of: (1) the *subset skill score* assessing the performance of a forecast system compared to a reference system for a particular subset; (2) the *frequency weighting* accounting for varying subset size; (3) the *reference weighting* relating the performance of the reference system in the individual subsets to the performance of the full data set. The decomposition and its interpretation is exemplified using synthetic data. Subsequently we use it for a practical example from the field of decadal climate prediction: An evaluation of the Atlantic-European near-surface temperature forecast from the German initiative Mittelfristige Klimaprognosen (MiKlip) decadal prediction system conditional on different Atlantic Multidecadal Oscillation (AMO) phases during initialization. With respect to the chosen Western European North Atlantic sector, the decadal prediction system *preop-dcpp-HR* performs better than the un-initialized simulations mostly due to contributions during the positive AMO phase driven by the subset skill score. Compared to the low-resolution system (*preop-LR*), no overall performance benefits are made in this region, but positive contributions are achieved for initialization in neutral AMO phases. Additionally, the decomposition reveals a strong imbalance among the subsets (defined by AMO phases) in terms of *reference weighting* allowing for insightful interpretation and conclusions. This skill score decomposition framework for conditional verification is a valuable tool to analyze the effect of physical processes on forecast performance and consequently supports model development and improvement of operational forecasts.

1 Introduction

The verification of forecast systems plays an important role in the field of weather and climate prediction to asses the quality of such systems and, moreover, of the entire forecast process. Furthermore, a common practice for evaluating forecast systems is the comparison against another competing prediction system or a standard reference forecast such as the persistence or climatological forecast. Basically, the relative performance in terms of accuracy of a prediction system with respect to a reference is expressed as forecast skill and is usually presented as a skill score (Wilks, 2011). Therefore, a variety of skill scores

are widely used for verification, e.g., the mean squared error skill score (MSESS) is a common way to verify a deterministic forecast, while the Brier skill score (BSS), the ranked probability skill score (RPSS) or the continuous ranked probability skill score (CRPSS), e.g., in decadal forecast verification (e.g., Kadow et al., 2016; Kruschke et al., 2016; Pasternack et al., 2018, 2021), could be the choice for a probabilistic forecast.

30   Since the forecast performance is typically not homogeneous in time and space, it is of interest how variable the forecast skill is for different states of the system. Therefore, conditional verification is a common practice in weather and climate research, i.e. the evaluation of forecasts separately for different regions (e.g., Northern Hemisphere and Southern Hemisphere) or seasons (e.g., winter and summer). Additionally, the initial state and particular conditions the system goes through during the forecast might also affect the prediction skill. In weather forecasting, the state of atmospheric flow regimes or circulation patterns can

35   influence the forecast quality (Grönås, 1982, 1985), where a more stable regime such as blocking can improve the forecast quality of a model (Tibaldi and Molteni, 1990). The presence of different climate states during the initialization procedure of medium-range forecasts, which can improve the predictive ability in certain periods, is addressed in the subseasonal-to-seasonal (S2S) prediction community (Mariotti et al., 2020). Large-scale atmospheric circulation variability, such as the North Atlantic Oscillation (NAO, Jones et al., 2004; Ferranti et al., 2015; Jones et al., 2015), the Madden-Julien Oscillation (MJO,

40   Ferranti et al., 2018) or circulation patterns (Frame et al., 2013; Richardson et al., 2021) as well as coupled ocean-atmospheric phenomena like El Niño–Southern Oscillation (ENSO, e.g., Qin and Robinson, 1995; Branković and Palmer, 2000; Goddard and Dilley, 2005; Frías et al., 2010; Kim et al., 2012; Manzanas et al., 2014; Miller and Wang, 2019) can contribute to a forecast skill improvement. In decadal climate prediction – the focus of this study – the state of the ocean has the potential to affect long-term forecasts of the following years, i.e. an enhanced subpolar ocean heat transport (OHT) linked to North

45   Atlantic upper ocean heat content (UOHC) and in some way via the Atlantic Meridional Overturning Circulation (AMOC) to the positive Atlantic Multidecadal Oscillation/Variability (AMO/AMV) phase shows the potential of an improved predictive ability during the initialization of a climate model (Müller et al., 2014; Zhang and Zhang, 2015; Borchert et al., 2018, 2019).

In a typical verification study, the accuracy of a given forecast is compared to a reference to evaluate the quality of the forecast. To assess the forecast quality for specific situations (states, seasons, regions, etc.) verification can be carried out

50   conditional on these situations by stratifying the full data set along situations. Thus the forecast data set is split up and (skill) scores are obtained individually for the splits. The interpretation of these partial skill scores is not necessarily straightforward. This is particularly the case when the reference strongly varies among individual subsets compared to the overall behavior and is commonly known as "Simpson's Paradox" (Pearson et al., 1899; Yule, 1903; Simpson, 1951; Blyth, 1972). With respect to weather and climate prediction, a potential mis-interpretation of the forecast performance stratified along specific conditions

55   or samples may arise if the underlying climatology that is used as reference forecast differs in some way among these samples (e.g., Murphy, 1996; Goeber et al., 2004; Hamill and Juras, 2006). In that case a fair comparison should consider the varying behavior of such climatology in the verification procedure.

While the majority of mentioned studies focus more on decomposing a skill score to measure basic aspects of forecast quality with respect to a climatological reference forecast in a fair way, here we apply a decomposition framework in the

60   context of conditional verification in the field of decadal predictions. The aim is to evaluate the performance of individual

subsets in relation to the performance of the entire forecast set. The decomposition provides a simple diagnostic tool to assess the contribution of certain subsets to the overall skill as well as to identify potential causes of variable skill between these subsets. The resulting information can be further used to analyze physical processes related to certain subsets and consequently to support the model development and to optimize operational forecasts. In terms of decadal forecasts, we exploit the potential source of long-term predictability forced by ocean states associated with the AMO to improve the forecast assessment.

First, the general decomposition procedure of the skill score is described in section 2 and exemplified in section 3 using synthetic data. In section 4, the decomposition is applied to decadal predictions to evaluate the Atlantic-European near-surface temperature forecast of a pre-operational forecast system depending on different North Atlantic ocean states. The latter are determined by the Atlantic Meridional Oscillation (AMO). The results are summarized and discussed in section 5. Section 6 concludes this study.

2 Decomposition of skill score

This section presents the decomposition of a skill score into contributions from different subsets derived from the full set of forecast-observation pairs and discusses the interpretation of individual terms.

2.1 Subset contribution

To verify a forecast f_n we calculate a verification score $\mathrm{S} = \mathrm{S}_n(f_n, o_n)$, an error metric between an individual forecast f_n and the corresponding observation o_n (Wilks, 2011). Considering all forecast-observation pairs $(f_n, o_n), n = \{1, \ldots, N\}$, the mean score $\overline{\mathrm{S}}$ of the full set can be computed by

$$\overline{\mathrm{S}} = \frac{1}{N} \sum_{n=1}^{N} \mathrm{S}_n = \sum_{i=1}^{K} \frac{N_i}{N} \left(\frac{1}{N_i} \sum_{n=1}^{N_i} \mathrm{S}_n \right) = \sum_{i=1}^{K} \frac{N_i}{N} \overline{\mathrm{S}}_i \tag{1}$$

with $N = N_1 + \ldots + N_K$, where K is number of non-overlapping subsets i of the data, N_i the number of forecast-observation pairs in subset i and N the total number of forecast-observation pairs.

The mean squared error (MSE) is an adequate score for a deterministic forecast of a continuous variable, while the ranked probability score (RPS) is an appropriate choice for a probabilistic forecast of a discrete forecast. To measure the performance of a forecast system *fc* compared to a reference forecast *ref*, the associated skill score SS (e.g., MSE skill score MSESS and ranked probability skill score RPSS, respectively) is used.

The forecast performance may vary for individual subsets of the data and the resulting interpretation may depend on the different behavior of the reference system. To assess varying skill scores for specific situations (e.g., states, periods, seasons, regions), the verification is carried out conditional on these situations, i.e., the full data set is stratified. We thus split the data

into K subsets and determine the individual *subset contribution* of each subset i to the overall mean skill score SS

$$\text{SS} = \frac{\overline{S}^{\text{fc}} - \overline{S}^{\text{ref}}}{S^{\text{perf}} - \overline{S}^{\text{ref}}}$$

$$= \frac{\sum_{i=1}^{K} \frac{N_i}{N} \overline{S}_i^{\text{fc}} - \sum_{i=1}^{K} \frac{N_i}{N} \overline{S}_i^{\text{ref}}}{S^{\text{perf}} - \overline{S}^{\text{ref}}} \tag{2}$$

$$= \sum_{i=1}^{K} \underbrace{\frac{N_i}{N} \left(\frac{\overline{S}_i^{\text{fc}} - \overline{S}_i^{\text{ref}}}{S^{\text{perf}} - \overline{S}^{\text{ref}}} \right)}_{\text{contribution subset i}},$$

where $\overline{S}^{\text{fc}}$ and $\overline{S}^{\text{ref}}$ are the mean scores of the forecast system *fc* and the reference system *ref*, respectively, over an entire data set with N forecast-observation pairs and S^{perf} the score of a perfect forecast, which is 0 for the MSE or RPS. $\overline{S}_i^{\text{fc}}$ and $\overline{S}_i^{\text{ref}}$ represent the mean score of the forecast system and reference system, respectively, for individual subsets.

2.2 Terms of decomposition

In order to evaluate how strongly and in which situations the skill score of the subsets affects the total skill score, we include and separate any component that influences the contribution of a subset to the overall skill score. We multiply equation Eq. (2) by $1 = \frac{S^{\text{perf}} - \overline{S}_i^{\text{ref}}}{S^{\text{perf}} - \overline{S}_i^{\text{ref}}}$, yielding

$$\text{SS} = \sum_{i=1}^{K} \underbrace{\frac{N_i}{N}}_{\substack{\text{frequency} \\ \text{weighting}}} \cdot \underbrace{\left(\frac{\overline{S}_i^{\text{fc}} - \overline{S}_i^{\text{ref}}}{S^{\text{perf}} - \overline{S}_i^{\text{ref}}} \right)}_{\substack{\text{subset} \\ \text{skill score}}} \cdot \underbrace{\left(\frac{S^{\text{perf}} - \overline{S}_i^{\text{ref}}}{S^{\text{perf}} - \overline{S}^{\text{ref}}} \right)}_{\substack{\text{reference} \\ \text{weighting}}}$$

$$= \sum_{i=1}^{K} W_{\text{freq}_i} \cdot \text{SS}_i \cdot W_{\text{ref}_i} = \sum_{i=1}^{K} W_i \cdot \text{SS}_i. \tag{3}$$

The individual *subset contribution* $W_i\text{SS}_i$ of a certain subset to the overall skill score depends on i) SS_i the performance of the forecasting system compared to the reference system in that given subset, weighted by ii) W_{freq_i} the relative size of the subset (frequency of the stratification event occurring) and iii) W_{ref_i} the performance of the reference system in the subset compared to the full set of forecast-observation pairs.

In detail, SS_i is the mean *subset skill score* of the forecast system *fc* versus the reference system *ref* with respect to forecast-observation pairs of the given subset i. This term characterizes how well the forecast system performs in comparison to the reference system *in that specific subset*, e.g., during a positive AMO phase. It is commonly applied in model evaluations to find enhanced predictability during certain climate or large-scale circulation states or specific seasons.

W_{freq_i} is the *frequency weighting* and considers the number of forecast-observation pairs (e.g., time steps) in subset i relative to the total number of forecast-observation pairs. For a time series one could imagine, this part reflects the relative frequency of occurrence of the situation stratified along within the total time period.

W_{ref_i} is the *reference weighting* and defines the ratio of the mean score of the reference system for the subset i (numerator) and the full set of forecast-observation pairs (denominator). It adjusts the scale (or range) of the subset skill score which was set by $\mathrm{S}^{\mathrm{perf}} - \overline{\mathrm{S}}_i^{\mathrm{ref}}$ to the scale used for the overall skill score. This component can be interpreted as a weighting of the subset skill score by means of the performance of the reference system in the subset compared to its performance in the full set of forecast-observation pairs. If the performance of the reference varies strongly among subsets, the individual subset skill scores will contribute to the total skill score according to the performance of the reference.

The total subset weight W_i (product of the *frequency weighting* and the *reference weighting*) determines the influence of the subset skill score on the total skill score, i.e. for an improvement/degradation $\Delta \mathrm{SS}_i$ of the forecast in the subset i, the total skill score for the full set of forecast-observation pairs changes accordingly by

$$\Delta \mathrm{SS}_{(\Delta \mathrm{SS}_i)} = W_i \cdot \Delta \mathrm{SS}_i \,. \tag{4}$$

3 Synthetic cases

We illustrate the effect of the different reference performance using synthetic data in the following. In the context of near-term climate prediction one could imagine the annual mean of 2m-temperature being verified in two different forecast systems with respect to the same observation for a certain defined period.

3.1 Example cases with different behavior of skill scores

With respect to a time-based stratified verification which is addressed in this study, we assume that the performance of both forecast systems varies systematically within the period considered. For this purpose, we divide the entire period – here we use a period of $N = 60$ time steps representing 60 years – into two equal sized subsets ($K = 2$, $N_1 = N_2 = 30$). The performance of the two forecast systems shows a systematically different behavior for the two subsets. An example from near-term climate prediction could be the state of the ocean in terms of years dominated by a negative or positive AMO phase during the initialization procedure, which might have an influence on the forecast performance in some regions via the OHT (Borchert et al., 2018).

Applied to our fictive example, the mean scores of the reference systems differ between both subsets. In some situations it is possible that the long-term performance expressed in terms of total skill score SS of a forecast system compared to another forecast system is dominated by a specific subset period. With the setting described above and the decomposition approach from Sect. 2, we illustrate and discuss the individual contributions of subsets to the total skill score. For this purpose we generate six hypothetical cases with different performance combinations of forecast *fc* and reference *ref* during the two subsets $i = 1$ and $i = 2$. Three cases in setup *A* assume a very different performance of the reference system in the two subsets and three cases in setup *B* assume an almost equal performance of the reference instead. For simplicity, we set $\mathrm{S}^{\mathrm{perf}} = 0$.

Case	Skill score behavior	$\overline{S}_1^{fc}$	$\overline{S}_1^{ref}$	**SS$_1$**	$\overline{S}_2^{fc}$	$\overline{S}_2^{ref}$	**SS$_2$**	$\overline{S}^{fc}$	$\overline{S}^{ref}$	**SS**
A0	SS$_1$ better than SS$_2$; SS close to SS$_2$	0.22	0.26	**0.15**	2.48	2.70	**0.08**	1.35	1.48	**0.09**
A1	SS$_1$: increase; SS: nearly unchanged	0.11	0.26	**0.58**	2.48	2.70	**0.08**	1.29	1.48	**0.13**
A2	SS$_2$: increase; SS: increase	0.22	0.26	**0.15**	1.24	2.70	**0.54**	0.73	1.48	**0.51**

Table 1. Cases of setup *A* (*A0-A2*) showing the mean scores ($\overline{S}$) and skill scores (SS) of two subsets and of the total forecasts. The influence of the skill score in subset 1 on the total skill score is weak compared to the one of subset 2. The skill score changes as described in *A1* and *A2*, both related to the first case *A0*.

3.1.1 Setup A: Unequal performance of the reference

In the base case of setup *A* (*A0*, see Table 1) we assume the forecast system *fc* performs better compared to the reference in subset $i = 1$ (subset skill score SS$_1 = 0.15$). In subset $i = 2$, the forecast system *fc* performs slightly poorer compared to the first subset (SS$_2 = 0.08$). Following the "Simpson's Paradox", from seeing the skill scores one might be tempted to think the total skill score SS being an equal composition (e.g., arithmetic mean) of both subset skill scores SS$_{1/2}$. However, in this specific configuration the total skill score of the overall data (SS $= 0.09$) is very close to that one in subset 2. The total skill of forecast system *fc* is mainly dominated by this subset.

The next scenario will be covered in case *A1* (Table 1) where an improvement of the subset skill score is achieved for the first subset by improving the error metric, i.e. reducing the mean score of the forecast system $\overline{S}_1^{fc}$ to the half, while the mean score and skill score of the second subset remain the same. Although the skill score of the forecast system *fc* in subset $i = 1$ is improved (*A1*: SS$_1 = 0.58$), the overall skill score hardly changes (*A1*: SS $= 0.13$). In contrast, in the last case (*A2* in Table 1) we set a similar improvement of the skill score in subset $i = 2$ (SS$_2 = 0.54$). Here, the total skill score (SS $= 0.51$) increases considerably more compared to *A1*.

Taking into account all three cases, it can be summarized that the total skill score of the forecast system *fc* with respect to the reference *ref* is mainly dominated by the subset skill score from subset $i = 2$; to be seen in Fig. 1a, where the overall skill score of the full set of forecast-observation pairs (gray bars) behaves very sensitively towards changes in the subset skill score from subset $i = 2$ (orange), whereas changes of the skill score from subset $i = 1$ (green) yield almost no effect.

3.1.2 Setup B: Equal performance of the reference

In contrast to setup *A*, in setup *B* we show three related examples (*B0-B2* in Table 2) in which the influence on the total skill score is nearly equally balanced between both subsets. To see the different behavior, the subset skill scores and the relative sizes of the score improvements in *fc* of all cases will be the same as before. Consequently, in the base case of setup *B* (*B0* in Table 2) the forecast system *fc* performs better in subset $i = 1$ compared to the reference system *ref* (SS$_1 = 0.15$), while it shows a weaker performance in subset $i = 2$ (SS$_2 = 0.08$). Unlike case *A0*, the total skill score now depends almost equally on
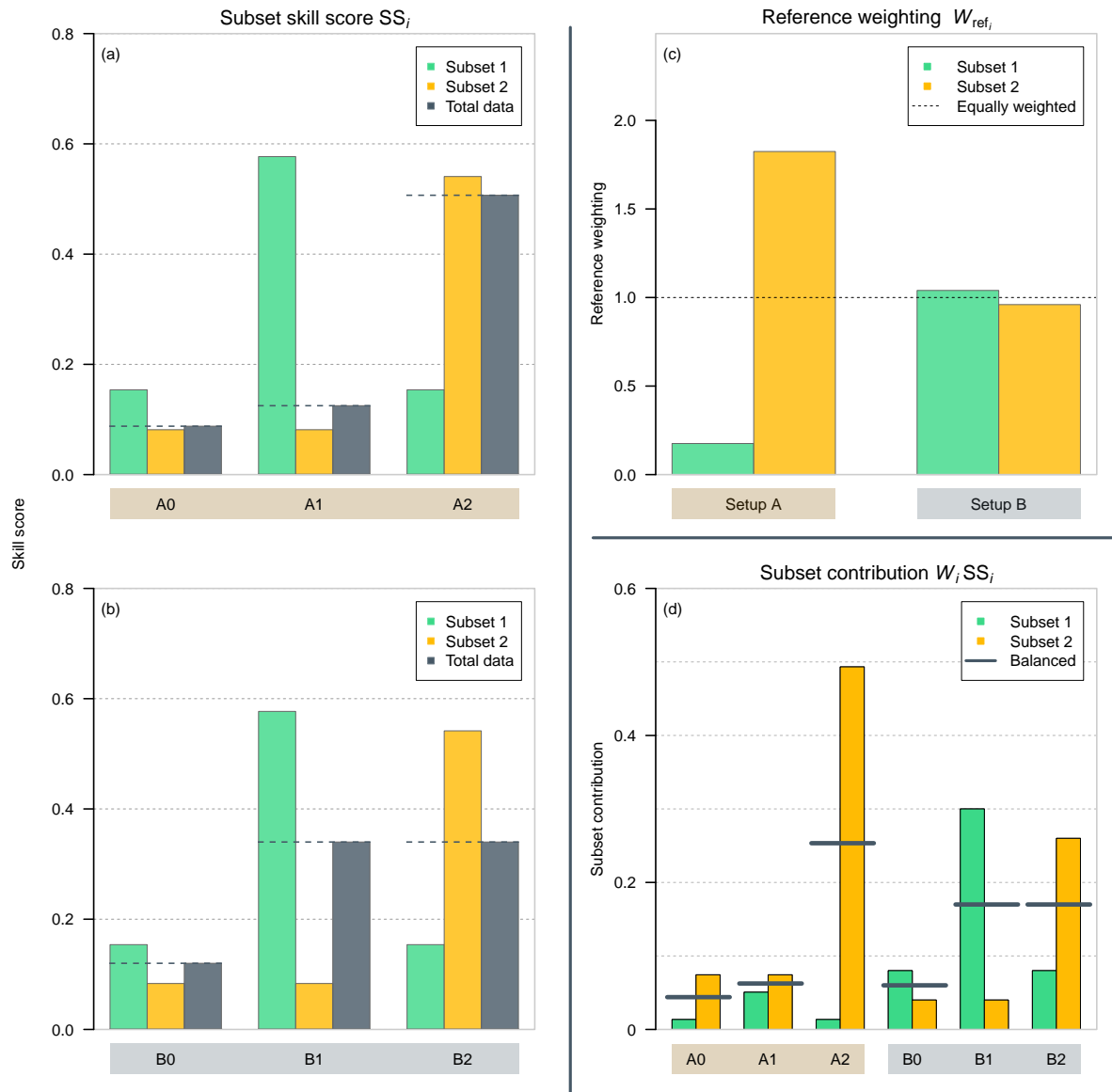
Figure 1. (a,b) Subset skill scores (green/orange bars) and their influence on the respective total skill score (gray bars and dashed lines) from synthetic example cases of (a) setup *A* (brown background) shown in Table 1 (strong reference weighting imbalance among both subsets) and (b) setup *B* (gray background) shown in Table 2 (nearly balanced reference weighting among both subsets). (c) Reference weighting of both subsets (green/orange bars) for setup *A* and *B*. The dashed line reflects a balanced behavior among both subsets. (d) Subset contributions of both subsets (green/orange bars) from cases of setup *A* and setup *B*. Gray horizontal lines indicate a balanced contribution SS_{bal} (see Sect. 3.3) with respect to the total skill score.

Case	Skill score behavior	$\overline{S}_1^{\mathrm{fc}}$	$\overline{S}_1^{\mathrm{ref}}$	$\mathbf{SS_1}$	$\overline{S}_2^{\mathrm{fc}}$	$\overline{S}_2^{\mathrm{ref}}$	$\mathbf{SS_2}$	$\overline{S}^{\mathrm{fc}}$	$\overline{S}^{\mathrm{ref}}$	$\mathbf{SS}$
B0	SS$_1$ better than SS$_2$; SS nearly centered of SS$_1$ and SS$_2$	0.22	0.26	**0.15**	0.22	0.24	**0.08**	0.22	0.25	**0.12**
B1	SS$_1$: increase; SS nearly centered of SS$_1$ and SS$_2$	0.11	0.26	**0.58**	0.22	0.24	**0.08**	0.16	0.25	**0.34**
B2	SS$_2$: increase; SS nearly centered of SS$_1$ and SS$_2$	0.22	0.26	**0.15**	0.11	0.24	**0.54**	0.16	0.25	**0.34**

Table 2. Cases of setup *B* (*B0-B2*) similar to table 1, but in contrast the influence of the skill score of subset 1 and subset 2 on the total skill score is similar.

both subsets (SS $= 0.12$). The changes made to the two cases *B1* and *B2* follow a similar pattern as the changes in *A1* and *A2* as can be seen in Fig. 1b, whereas the total skill score is almost given by the arithmetic mean of both periods.

With the skill score decomposition from Sect. 2 the reason for this behavior can be investigated.

3.2 Decomposition of skill scores and impact of the reference weighting

The different behaviors shown can be investigated using the decomposition terms from Eq. (3) with $S^{\mathrm{perf}} = 0$. As demonstrated there, the contribution of an individual subset to the total skill score depends on three terms: frequency weighting, reference weighting and the subset skill score. As defined above, we varied the subset skill scores in the same way and used equal-sized subsets resulting in the same frequency weighting of $\frac{1}{2}$ for both subsets. Consequently, the reference weighting for the individual subsets must play a crucial role. For setup *A* the mean scores ($\overline{S}_{1/2}$) between subsets differ by more than one unit. In detail, the scores generally are much higher in subset $i = 2$ than in subset $i = 1$. As a result, potential subset skill score changes for the forecast system *fc* that are just achieved during the first subset will not affect the total skill score very much. The larger scores in subset $i = 2$ show a stronger relevance with respect to the total skill.

In contrast to setup *A*, setup *B* shows a nearly balanced behavior in this respect. These difference can also be seen when we compare the reference weighting term from the skill score decomposition described before. Figure 1c visualizes this behavior, in which the cases from setup *A* show a different value for the reference weighting in both subsets, while in setup *B* the reference weighting is close to 1 in both cases.

Generally, the reference weighting lies between 0 and K (number of subsets). Values below (above) 1 reflect a lower (higher) than average contribution to the overall skill score. Figure 2 demonstrates the impact of individual subset skill scores on the resulting total skill score depending on their reference weighting. We compute the total skill score SS with respect to our cases (Fig. 2b) with prescribed subset skill score in subset $i = 1$ (SS$_1$) and subset $i = 2$ (SS$_2$), respectively, and change successively the reference weighting term (Fig. 2a). Starting with a behavior similar to the setup *A* which is dominated by subset $i = 2$ (left in Fig. 2), where the reference weighting term of subset $i = 2$ (orange bars) is larger than the one of subset $i = 1$ (green). A balanced ratio between both subsets (similar to setup *B*) is shown in the middle. The right part shows a total skill score which is mainly controlled by the subset $i = 1$. Thus, the reference weighting controls the subset's contribution to the overall skill score.
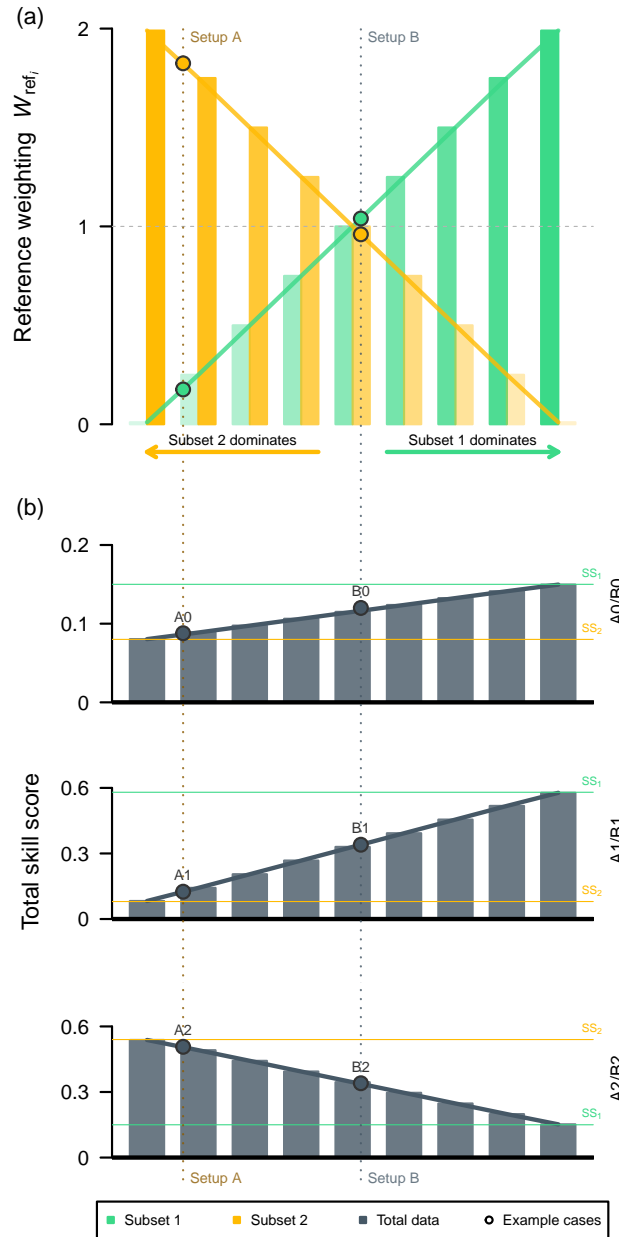
Figure 2. (a) Variations in the reference weighting term of both subsets (green/orange bars) and (b) their potential influence on the corresponding total skill score (gray bars) for given subset skill scores $SS_{1/2}$ (green/orange horizontal lines) from example cases of setup *A* (*A0-A2*) described in Table 1 and setup *B* (*B0-B2*) in Table 2. Current values of the example cases are highlighted with a dot. A balanced (enhanced unbalanced) behavior among both subsets reflects the center bar pair (bar pairs towards left/rights edges).

ΔSS_1	ΔSS_2	$\Delta \mathbf{SS}$	$W_{\mathrm{ref},1}$	$W_{\mathrm{ref},2}$	$W_{\mathrm{freq},1/2}$
0.5	0	**0.045**	0.18	1.82	0.5
0	0.5	**0.455**	0.18	1.82	0.5

Table 3. Individual effect of a 0.5 change in the subset skill score SS_i on the total skill score SS for setup *A*. The weighting terms from the decomposition are also shown.

According to Eq. (4), we can compute potential changes of the total skill score ΔSS depending on changes in the subset skill score ΔSS_i. For example, in setup *A* a change of the subset skill score in subset $i = 1$ of $\Delta SS_1 = 0.5$ would change the total skill score of only $\Delta SS = 0.045$. On the other hand, a skill gain of 0.5 in subset $i = 2$ would increase the total skill score by a value of 0.455. In detail, with $S^{\mathrm{perf}} = 0$ the derived weighting terms from the decomposition are shown in Table 3. In this example, it is more effective in terms of gain in total skill score to focus on the subset $i = 2$ for improvement of the forecast system.

The synthetic example is focused on the reference weighting; however the decomposition is also useful for unequal subset sizes. The contribution to the total skill score is then additionally controlled by the frequency weighting. Depending on the verification setup, both parts should be considered in weather and climate forecasts. As a consequence, complexity is reduced when each subset has the same size and the reference weighting of all subsets is 1 due to a chosen reference. This leads to equally weighted skill scores of the subsets.

3.3 Subset contributions

In Fig. 1d, we assess the subset contributions compared to a balanced contribution across the synthetic example cases. The balanced contribution (gray horizontal lines) represents a hypothetical value resulting from distributing the total skill score into equal contributions from the K subsets: $SS_{\mathrm{bal}} = \frac{SS}{K}$. The sign of the subset contribution indicates positive or negative contribution to the total skill score, while its value indicates the amount of the contribution. In setup *A*, the values of the contribution from subset 2 (orange bars) are larger than the contributions of subset 1 (green bars), even for cases where the subset skill score SS_1 is higher (*A0* and *A1*, Fig. 1a). In setup *B* the contributions behave similar to the subset skill scores. Strongly differing deviations from SS_{bal} between the subsets show the strong imbalance between the contributions of both subsets. Since, the frequency weighting of both subsets is identical, the observed characteristic is driven by the reference weightings.

In summary, the decomposition of the subset contribution into its three components reveals the potential impact of a subset on the overall skill score considering the combination of all three terms of the subset (i.e., size and performance of the reference) instead of only the skill score for a particular subset.

4 Conditional verification in the MiKlip decadal prediction system

4.1 Simulations from MiKlip decadal prediction system

We investigate the influence of ocean states – given in terms of AMO phases – on the near-surface air temperature hindcast skill in the MiKlip decadal climate prediction system. The MiKlip decadal climate prediction system (Marotzke et al., 2016) generation *preop-dcpp* is based on the coupled atmosphere-ocean Earth System Model of the Max-Planck Institute version 1.2 simulated in the high-resolution setting *HR* (Müller et al., 2018; Mauritsen et al., 2019). The model for the atmospheric component – ECHAM6.3 – has a T127 horizontal resolution ($0.9375°$) and 95 vertical levels. The ocean part is simulated by the Max Planck Institute ocean model (MPIOM) with a horizontal resolution of $0.4°$ and 40 vertical levels.

The 10-member ensemble of the system is initialized on an annual basis from 1960 to 2012, with a period of 10 years being simulated for each run. The initialization procedure is similar to Pohlmann et al. (2013) which is based on nudging the model toward atmospheric and oceanic fields obtained from reanalysis data. In case of the atmospheric model component, a full atmospheric field-initialization from ERA40 (Uppala et al., 2005) and Era-Interim (Dee et al., 2011) reanalyses is applied. For the ocean component, salinity and ocean temperature anomalies derived from an assimilation experiment forced by ORA-S4 ocean reanalysis data (Balmaseda et al., 2013) as well as sea ice concentrations from the National Snow and Ice Data Center (Fetterer et al., 2018) described in Bunzel et al. (2016) are taken as initial conditions. The external forcing is based on the CMIP6 forcing (see Eyring et al. (2016) and Pohlmann et al. (2019) for details). In addition to the initialized simulations, an ensemble of 10 un-initialized runs (historical simulations) is used as the competitive prediction for the skill assessment. Further details about the simulations can be found in Müller et al. (2018) and Pohlmann et al. (2019). To evaluate the probabilistic hindcast skill, both sets of predictions are verified against observations from the Hadley Centre and Climate Research Unit (HadCRUT4, Morice et al., 2012). To be on the same horizontal resolution as the observational data, the model data of the prediction system is re-gridded to a regular $5° \times 5°$ grid.

4.2 Atlantic Multidecadal Oscillation time series

Since the multi-decadal variability of the ocean state in the North Atlantic (e.g., AMV, AMOC, OHT) is represented in the decadal prediction system and shows predictive potential (Müller et al., 2014; Borchert et al., 2018, 2019; Höschel et al., 2019), we will apply the conditional verification of the temperature stratified along three different phases of the Atlantic Multidecadal Oscillation (AMO). We calculate the AMO index proposed by Enfield et al. (2001) in the ORA-S4 ocean reanalysis data to match the current state of the Atlantic ocean during the initialization procedure. Specifically, monthly anomalies (base period: 1960–2010) of the sea surface temperature (SST) averaged over the North-Atlantic region (80–0° W, 0–60° N) are exploited to compute the North-Atlantic temperature time series. Afterwards, the linear trend (base period: 1960–2010) of this time series is removed to obtain the AMO time series. With regard to the subsequent conditional evaluation of the decadal prediction system, annual averages of the AMO are used to split the entire period into three different subsets (based on $0 \pm 0.5\sigma$ thresholds using base period 1960-2010) representing years of negative, neutral and positive AMO phases.

4.3 Verification of probabilistic forecasts for three categories

We verify the decadal ensemble predictions using the ranked probability score RPS (e.g., Wilks, 2011; Kruschke et al., 2016). The score is computed for both sets of predictions against the HadCRUT4 observation to asses the probabilistic skill of the initialized vs un-initialized simulations. For near-surface air temperature, we build time series of forecast-observation pairs depending on lead-time for all initialized decadal experiments from 1960 to 2012. Temperature data with lead-times between 2 and 5 years are averaged to compute a score for the lead-time period 2–5 years.

In the next step we divide the resulting data sets (separately for initialized, un-initialized and observational data) along their terciles into three equal parts to obtain $J = 3$ different temperature categories $j = 1, \ldots, J$ (below normal, normal, above normal). For both simulation data sets, the entire ensemble is used to determine the respective terciles. With this approach, an implicit lead-time-dependent bias-correction, which is commonly applied in decadal climate predictions projects, will be achieved.

The ranked probability score (RPS) defined as

$$\text{RPS}_t = \sum_{j=1}^{J} (Y_{j,t} - O_{j,t})^2 \tag{5}$$

is calculated between both sets of predictions and the observational data, where $Y_{j,t}$ is the cumulative forecast probability of class j (with $J = 3$) derived from the forecast ensemble of initialization year t for the given forecast lead-time mean 2–5 years by counting the ensemble members in each category and then dividing by the ensemble size. $O_{j,t}$ represents the corresponding observed cumulative probability represented as the Heaviside step function where either $O_{j,t} = 0$ in case a higher category than j is observed or $O_{j,t} = 1$ otherwise. To asses the skill between the initialized (*fc*) and un-initialized (*ref*) simulations, the ranked probability skill score

$$\text{RPSS} = 1 - \frac{\overline{\text{RPS}}_{\text{fc}}}{\overline{\text{RPS}}_{\text{ref}}} \tag{6}$$

is computed.

With respect to the conditional verification using the decomposition of the skill score, here we want to evaluate the probabilistic hindcast skill stratified along three phases (negative, neutral, positive) of the AMO instead of two demonstrated in Sect. 2. That means, the RPS and RPSS of the entire period contain every initialization year t from 1960 to 2012 as time step, while the AMO-phase-specific terms only consider initialization years which are related to the associated AMO phase.

The information about the significance of the RPSS is based on a 5-year-block-bootstrap method by a 1000-fold re-sampling of the forecast-reference-observation cases in the entire period. The RPSS value is considered statistically significant if 0 is outside the 95 % inner values of the bootstrap distribution.

A large part of the routines used for verification presented here is implemented as the verification plug-in *ProblEMS* (https://www.xces.dkrz.de/plugins/problems/detail/; via guest login; last access: 29 July 2024) into the MiKlip and ClimXtreme (https://www.xces.dkrz.de; last access: 29 July 2024) and ComingDecade Central Evaluation System (https://codes.dkrz.de;

last access: 29 July 2024) – based on the Free Evaluation System Framework for Earth System Modeling (Freva; Kadow et al., 2021).

4.4 Subset contributions of RPSS

Figure 3a shows the RPSS over the European region for the decadal hindcast with respect to the un-initialized simulations averaged over the entire hindcast period for lead-years 2–5. Significant values (marked with a cross) are rare. Negative significant values can be found in the Barents Sea and a larger patch in the south-western North Atlantic. The latter is presumably caused by a displacement of ocean currents in that area since the region is especially sensitive to initializations (Kröger et al., 2018; Polkova et al., 2019). Positive significant skill can be found in the Greenland Sea. Besides individual grid points with significant values, patches with positive but non-significant skill are visible in the eastern Mediterranean and in the north-eastern part of the North Atlantic.

To exemplify the stratified verification, Fig. 3b-d show the subset contributions $W_i\mathrm{SS}_i$ to the total RPSS during (b) negative, (c) neutral and (d) positive AMO phases at the time of the initialization following Eq. (3). Significances are computed as for the RPSS, but with 1-year-block-bootstrapping in the related subset period. AMO neutral phase (Fig. 3c) contributes to negative (positive) RPSS in the south-western North Atlantic and Barents Sea (Western European North Atlantic), while positive significant contributions in Western Europe (W-EU) and Central Europe (C-EU) are found during negative AMO phase (Fig. 3b) as well as in the North Atlantic under positive AMO conditions during the initialization procedure (Fig. 3d).

4.5 Decomposition of RPSS over Western European North Atlantic

Next, we focus on the Western European North Atlantic region (W-EU NA). This is motivated on the one hand by the different predictability associated with certain states of the ocean identified in previous studies (Zhang and Zhang, 2015; Borchert et al., 2018, 2019), and on the other hand by the positive total skill found in that region. We investigate the subset contributions $W_i\mathrm{SS}_i$ and the three terms (subset skill score SS_i, frequency weighting W_{freq_i}, reference weighting W_{ref_i}) of the decomposition for the annual field-mean of the W-EU NA region 40–10° W, 35–60° N, (box in Fig. 3) according to Eq. (2) and (3). The subset skill score (subset RPSS) in Fig. 4b shows no or at most very weak improvement of the initialized prediction system over the un-initialized simulations under negative and neutral AMO conditions during the initialization procedure. In contrast, the subset RPSS = 0.3 for initialization during positive AMO years. As comparison, the total RPSS is around 0.1 (gray horizontal line). The frequency weighting (Fig. 4c) indicates that initialization years with neutral AMO phase are more frequent (0.4) than years of the other two phases. This leads to a higher frequency weighting factor associated with the AMO neutral phase. Figure 4d shows that the reference weighting is close to 1 for all phases. As this component represents a potentially different score of the reference system along the three subsets, we do not expect large variability as the un-initialized reference is not influenced by the AMO phases in the observations.

Multiplying the three components for the individual subsets, we arrive at the subset contributions $W_i\mathrm{SS}_i$ (Fig. 4a). Although the contributions show large uncertainties and are not statistically significant, tendencies can be derived. The contribution is mainly determined by the subset skill score (Fig. 4b) and to a small extent modified by the frequency weighting (Fig. 4c). The
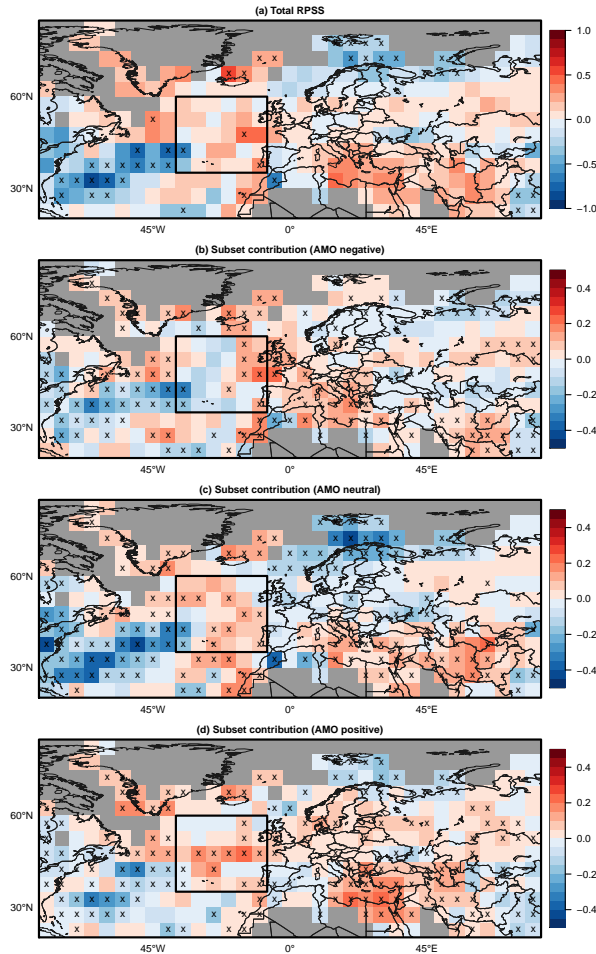
Figure 3. (a) Total ranked probability skill score (RPSS) of near-surface temperature of the initialized decadal simulations (*preop-dcpp-HR*) with respect to un-initialized historical simulations and HadCRUT4 observations for lead-year 2–5 from 1962–2017. Additionally, individual subset contributions $W_i SS_i$ for (b) negative, (c) neutral and (d) positive AMO phase at the time of the initialization. Missing values are depicted in gray. Crosses indicate areas with significant (95 %-level) values. The box highlights the W-EU NA region analyzed in Sect. 4.5.

resulting subset contributions related to the AMO phases show that the positive AMO phase contributes the most (around 0.08) to the total RPSS, followed by the neutral AMO phase with a much smaller contribution of 0.02.

Since the reference weighting was not relevant in the above case, we now choose a reference system affected by the AMO phase: a lower-resolution version of the decadal prediction system. The pre-operational version *preop* in a low-resolution configuration *LR* has a T63 horizontal grid ($1.875°$) and 47 vertical levels in the atmospheric component, while the ocean part has a horizontal resolution of $1.5°$ and 40 vertical levels. Being an older version, the low-resolution system is forced by CMIP5 external forcing (Giorgetta et al., 2013). The other settings (e.g., initialization and assimilation procedure etc.) remain
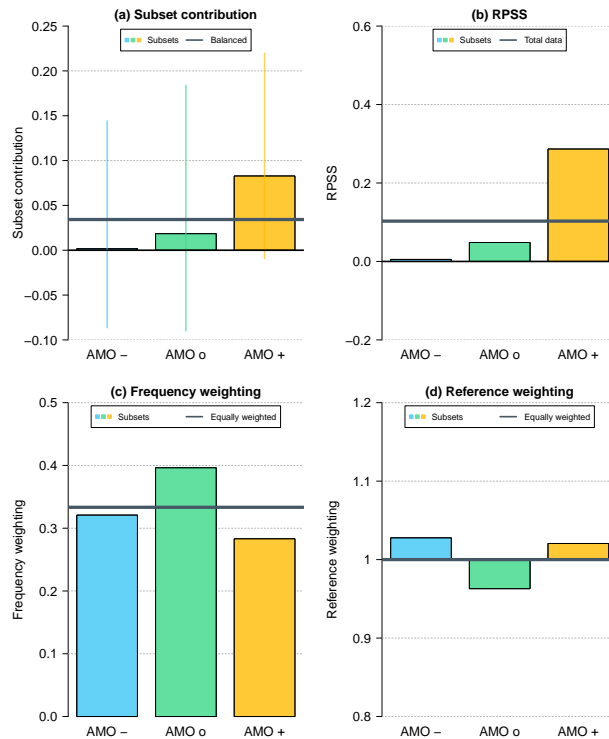
Figure 4. (a) Subset contributions (95 %-confidence intervals as vertical segments) related to Eq. (2) as well as (b) subset RPSS, (c) frequency weighting and (d) reference weighting of subsets (defined by AMO phase during the initialization) according to Eq. (3) for the conditional verification of near-surface temperature in the W-EU NA region between initialized decadal simulations (*preop-dcpp-HR*) and un-initialized historical simulations with respect to HadCRUT4 observations for lead-year 2-5 from 1962-2017. Gray horizontal lines represent (b) total skill score, (c–d) balanced weightings and (a) balanced contributions with respect to the total skill score.

unchanged compared to the *preop-dcpp-HR* version introduced in Sect. 4.1. Figure 5b shows again the RPSS of the individual subsets (bars) and the total RPSS as horizontal gray line. As the latter coincides with the zero skill score line, we see that the initialized prediction system *preop-dcpp-HR* does not outperform the low-resolution version *preop-LR* over the entire period. The subset RPSS under positive AMO conditions during the initialization procedure is strongly negative (-0.55); a similar tendency can be seen during the negative phase (-0.2). Only during the neutral AMO phase, the *preop-dcpp-HR* shows an improvement compared to the low-resolution version.

Since classification of AMO phases is again based on ORA-S4, the frequency weighting terms are the same as in the previous case. Again, the weighting factor of the neutral AMO phase is slightly higher than that of the other two phases (Fig. 5c). The reference weighting exhibits huge differences among the individual phases (Fig. 5d). While the subset of the neutral AMO phase shows a weighting factor of 1.4, which is approximately 40 % higher than the balanced value (1, gray horizontal line),
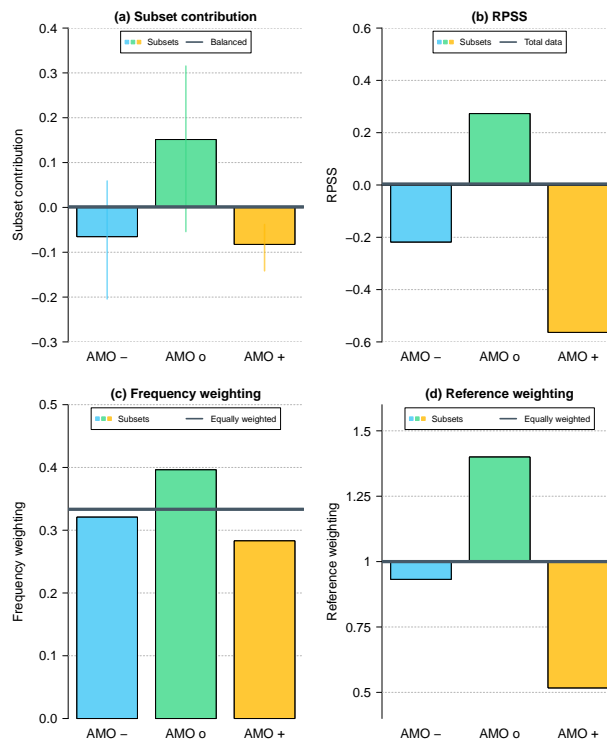
Figure 5. Same as Fig. 4, but with the *preop-LR* initialized prediction system as reference.

the reference weighting term of the subset of the positive phase is 0.5 and thus only half of the balanced one. The reference weighting associated to the negative AMO phase (0.9) lies in between.

The individual subset contributions (Fig. 5a) are now affected by all three terms of the skill score decomposition. In particular, the reference weighting now influences the contribution to a large extent. While the subset RPSS (Fig. 5b) suggests a strong negative contribution to the overall skill driven by a positive AMO phase alone, the subset contribution (Fig. 5a) allows a slightly different interpretation: positive (statistically significant) as well as negative AMO phases contribute negatively to the overall skill score with similar amounts, counteracting the benefits from the neutral AMO phase.

5 Summary and discussion

We present a decomposition of skill scores into contributions from subsets of the forecasts which are selected according to characteristics of processes or large scale circulation, climate states during initialization of the forecast system, seasons or regions. We give examples for this decomposition in the context of synthetic data designed to reveal situations where this decomposition shows its usefulness. To achieve this, the synthetic cases show different performance characteristics of forecast and reference systems in two subsets. These subsets contribute differently to the overall skill score in an additive way; according

to their size, the performance of the forecast system on the subset and the performance of the reference system on the subset compared to the full data set. Hence, the *subset contribution* of a specific subset to the overall skill can be decomposed into

subset skill score $\mathrm{SS}_i = \frac{\overline{S}_i^{\mathrm{fc}} - \overline{S}_i^{\mathrm{ref}}}{S^{\mathrm{perf}} - \overline{S}_i^{\mathrm{ref}}}$,

frequency weighting $W_{\mathrm{freq}_i} = \frac{N_i}{N}$,

340   **reference weighting** $W_{\mathrm{ref}_i} = \frac{S^{\mathrm{perf}} - \overline{S}_i^{\mathrm{ref}}}{S^{\mathrm{perf}} - \overline{S}^{\mathrm{ref}}}$.

The *subset skill score* measures the performance of a forecast system compared to a reference system for a particular subset, a useful and popular quantity to assess varying performance of a forecast system over different subsets; this is frequently used to detect enhanced/reduced predictability for certain climate and large-scale circulation states or specific seasons and regions (see references mentioned in the introduction). The *frequency weighting* reflects the size of the subset with respect to the full data

345   set. For small subsets, it reduces the subset's contribution to the overall skill and vice versa for large subsets. The *reference weighting* adjusts the scale (or range) of the skill score, which is set by the difference between the reference performance of the subset and the perfect forecast, to the scale relevant for the overall data set. For negatively oriented scores with $S^{\mathrm{perf}} = 0$, this is expressed by the ratio of the two differences, see Eq. (3). *Reference weighting* as well as *frequency weighting* are both independent of the forecast system. The product of all three terms yields the subset's contributions to the overall skill score.

350   We expect that this decomposition helps to avoid mis-interpreting a potential performance increase in a subset resulting, e.g. from a significant performance decrease in the reference system. In this context, climatological forecasts used as a reference system could also impact the interpretation of the skill, as discussed for example in Hamill and Juras (2006).

Subsequently, we exemplify the RPSS decomposition in the context of the MiKlip decadal prediction system stratified along characteristics of the AMO during forecast system initialization. The goal is the quantification of hindcast skill for the near-

355   surface air temperature for leadyear 2–5 over the North Atlantic and European region. The hindcasts (*preop-dcpp-HR*) show a weak positive overall skill (locally significant) in the north-eastern part of the North Atlantic and in the eastern Mediterranean compared to un-initialized historical simulations. Stratified verification along positive, negative and neutral AMO phases for initialization reveals

- a negative subset contribution to the total RPSS in the south-western North Atlantic and Scandinavia for a subset associ-
360   ated with neutral AMO and

- a positive subset contribution for W-EU and C-EU (AMO-) and in the North Atlantic (AMO+) for subsets associated with negative and positive AMO.

Although not statistically significant, the decomposition for the Western European North Atlantic box shows that the subset associated with a positive AMO phase at the time of the initialization contributes to the positive total RPSS with a positive

365   subset skill score only slightly modified by the frequency weighting. The latter findings are similar to those from Borchert et al. (2018) since AMO/AMV phases are linked to OHT with a lag of 5-10 years. Nevertheless, a stratification along different OHT states may strengthen the distinction between each subsets.

Additionally, evaluation of the decadal hindcast system versus a low-resolution version (*preop-LR*) shows that individual subset contributions being affected by all three terms of the decomposition, with the reference weighting playing a particular role. This leads to a slightly different conclusion: While the subset RPSS suggests that the strong negative contribution to the overall skill is mainly driven by positive AMO initialization, the decomposition reveals that both, the negative as well as the positive AMO phases contribute negatively with the same amount, counteracting the benefits from the neutral AMO phase.

Since our study does not fully account for uncertainties and the results are partly sensitive to the defined W-EU NA region and the chosen AMO index representing the ocean state (see supplementary material), further indices and sensitivity studies including the consideration of uncertainties can be applied for a more robust analysis. As this paper focuses on suggesting the framework of skill score decomposition for stratified verification demonstrated as a potential application in decadal predictions, detailed and robust analysis of physical processes being responsible for varying skill is beyond the scope of this study.

6   Conclusions

The verification of forecast systems stratified along characteristics of physical processes, large-scale circulation, climate states at initialization, seasons or regions can be a helpful tool for model development, the detailed assessment of forecasts quality, as well as for communication of forecasts. However, interpretation and comparison of skill scores across different strata can be challenging. This is not only the case for different subset sizes (*frequency weighting*) but also if the performance of the reference system varies strongly across subsets (*reference weighting*).

Both examples, the synthetic data, as well as the one from decadal forecasting, exemplify the potential of the skill score decomposition for stratified verification. For the decadal prediction system, we see the strongest degradation of performance compared to its low-resolution system if it is initialized during positive AMO phases. However, the error of the reference system compared to observation in that subset is small compared to the entire time series (as can be seen in the lower reference weighting). As a consequence, the positive AMO phase negatively contributes to the overall performance nearly with the same amount as the negative AMO phase, although the subset skill score is much worse. In practice, potential model diagnostics and improvements should focus on both phases, rather than examining only the positive AMO phase suggested by the subset skill score assessment alone.

Assuming the reference score could measure inherent predictability with a mildly skillful reference, we would benefit more from improvements in subsets/situations with limited predictability (higher reference weighting) in terms of the overall skill. In contrast, improvements in situation with higher predictability have less effect on the total skill. However, it can be more difficult to improve the skill (of equal relative size) in these situations as the processes and drivers increasing the predictability may not be present or have less impacts. Accordingly, the decomposition can help to balance the aspects in order to support the assessment for a decision. Outside of the field of decadal predictions, the simultaneous investigation of the terms could be useful to evaluate and interpret regionally (e.g., between mountains and low-lands) or seasonally varying error behaviors with respect to the total model performance. A possible application is shown in Peter et al. (2024) using the example of the evaluation of statistical models for extreme precipitation.

The skill score decomposition into contributions from suitable chosen subsets helps understanding possible model mis-behavior in a detailed and robust way as subsets can be chosen along the characteristics of physical processes. This yields valuable information for refinement of the forecast system or model development. Besides the state of the ocean or other large-scale conditions, seasonal as well as regional or other aspects can be addressed. Conditional or stratified verification can be used to investigate known or hypothetical linkages in the area of climate and weather forecasts including the ability to simulate and represent specific feedback mechanism. The example above examines the potential source of long-term predictability forced by certain ocean states associated with the AMO.

Finally, to support decision-making related to weather and climate, operational forecasts can be optimized by assessing and communicating its credibility in a more specific and situative way using stratified evaluation along conditions of initialization and the related skill score decomposition. Depending on the condition during initialization, forecast skill can be quantified and eventually the forecast can be rated as more precise, as addressed in Borchert et al. (2019). Similar is the identification of windows of opportunity for enhanced skill on subseasonal to decadal time scales (Mariotti et al., 2020). A potential application outside the domain of decadal prediction could be the identification and analysis of such a window. In weather forecasting, the conditional verification stratified along particular flow regime conditions (e.g., blocking) or along different states of MJO and ENSO in subseasonal-to-seasonal predictions could be reasonable. In the example from decadal forecasting, a better temperature forecast ability of the prediction system compared to the un-initialized one is achieved over parts of the North Atlantic for initialization during positive AMO phases.

The skill score decomposition framework suggested and exemplified in context of conditional or stratified verification is a relatively simple tool to analyze physical processes related to certain subsets and consequently supports the model development as well as the optimization of operational forecasts and their communication.

Code and data availability. The code used for the verification of decadal predictions is written in Shell and R and uses CDO. R is a GNU licensed free software from the R Project for Statistical Computing (http://www.r-project.org; last access: 11 January 2024). Climate Data Operators (CDO, https://code.mpimet.mpg.de/projects/cdo; last access: 11 January 2024) is open source and released under the 3-clause BSD License. It is implemented as a software routine (*ProblEMS* plug-in) in the Freva system (Kadow et al., 2021) at Deutsches Klimarechenzentrum (DKRZ) and is versioned in gitlab. The version 1.6.3 used in this study is publicly available at https://doi.org/10.5281/zenodo.10469658. Synthetic examples, simulation data used in the conditional verification, and computed AMO time series (including computational routines) are publicly available at https://doi.org/10.5281/zenodo.10471223. HadCRUT4 data is freely available at https://www.metoffice.gov.uk/hadobs/hadcrut4/data/current/gridded_fields/HadCRUT.4.6.0.0.median_netcdf.zip (last access: 11 January 2024) and ORA-S4 ocean reanalysis data at https://icdc.cen.uni-hamburg.de/thredds/aggregationOras4Catalog.html?dataset=oras4_temp_all (last access: 11 January 2024).

Author contributions. AR prepared the manuscript with contributions from HR and JG. AR computed analyses and produced figures. HR, JG and AR developed the concept of the methodology. HR acquired the funding. All authors reviewed and edited the manuscript.

Competing interests. The authors declare that they have no conflict of interest.

Acknowledgements. We acknowledge funding from the Federal Ministry of Education and Research in Germany (BMBF) through the
435 research project MiKlip II (grant number (FKZ): 01LP1520A) and ComingDecade–Sim2Use (grant number (FKZ): 01LP2327C). This study used resources of Deutsches Klimarechenzentrum (DKRZ) and accessed data and plug-ins trough the Central Evaluation System framework Freva (Kadow et al., 2021). We thank Jonas Bhend and the anonymous reviewer for their constructive feedback and suggestions that improved the manuscript.

References

440 Balmaseda, M. A., Mogensen, K., and Weaver, A. T.: Evaluation of the ECMWF ocean reanalysis system ORAS4, Quarterly Journal of the Royal Meteorological Society, 139, 1132–1161, ISSN 1477-870X, https://doi.org/10.1002/qj.2063, 2013.

Blyth, C. R.: On Simpson's Paradox and the Sure-Thing Principle, Journal of the American Statistical Association, 67, 364–366, https://doi.org/10.1080/01621459.1972.10482387, 1972.

Borchert, L. F., Müller, W. A., and Baehr, J.: Atlantic Ocean Heat Transport Influences Interannual-to-Decadal Surface Temperature Pre-
445 dictability in the North Atlantic Region, Journal of Climate, 31, 6763 – 6782, https://doi.org/10.1175/JCLI-D-17-0734.1, 2018.

Borchert, L. F., Düsterhus, A., Brune, S., Müller, W. A., and Baehr, J.: Forecast-Oriented Assessment of Decadal Hindcast Skill for North Atlantic SST, Geophysical Research Letters, 46, 11 444–11 454, https://doi.org/https://doi.org/10.1029/2019GL084758, 2019.

Branković, C. and Palmer, T. N.: Seasonal skill and predictability of ECMWF PROVOST ensembles, Quart. J. Roy. Meteor. Soc., 126, 2035–2067, https://doi.org/https://doi.org/10.1256/smsqj.56703, 2000.

450 Bunzel, F., Notz, D., Baehr, J., Müller, W. A., and Fröhlich, K.: Seasonal climate forecasts significantly affected by observational uncertainty of Arctic sea ice concentration, Geophysical Research Letters, 43, 852–859, https://doi.org/10.1002/2015GL066928, 2016.

Dee, D. P., Uppala, S. M., Simmons, A. J., Berrisford, P., Poli, P., Kobayashi, S., Andrae, U., Balmaseda, M. A., Balsamo, G., Bauer, P., Bechtold, P., Beljaars, A. C. M., van de Berg, L., Bidlot, J., Bormann, N., Delsol, C., Dragani, R., Fuentes, M., Geer, A. J., Haimberger, L., Healy, S. B., Hersbach, H., Hólm, E. V., Isaksen, L., Kållberg, P., Köhler, M., Matricardi, M., McNally, A. P., Monge-Sanz, B. M., Mor-
455 crette, J.-J., Park, B.-K., Peubey, C., de Rosnay, P., Tavolato, C., Thépaut, J.-N., and Vitart, F.: The ERA-Interim reanalysis: configuration and performance of the data assimilation system, Quarterly Journal of the Royal Meteorological Society, 137, 553–597, ISSN 1477-870X, https://doi.org/10.1002/qj.828, 2011.

Enfield, D. B., Mestas-Nuñez, A. M., and Trimble, P. J.: The Atlantic Multidecadal Oscillation and its relation to rainfall and river flows in the continental U.S., Geophysical Research Letters, 28, 2077–2080, https://doi.org/10.1029/2000GL012745, 2001.

460 Eyring, V., Bony, S., Meehl, G. A., Senior, C. A., Stevens, B., Stouffer, R. J., and Taylor, K. E.: Overview of the Coupled Model Intercomparison Project Phase 6 (CMIP6) experimental design and organization, Geoscientific Model Development, 9, 1937–1958, https://doi.org/10.5194/gmd-9-1937-2016, 2016.

Ferranti, L., Corti, S., and Janousek, M.: Flow-dependent verification of the ECMWF ensemble over the Euro-Atlantic sector, Quarterly Journal of the Royal Meteorological Society, 141, 916–924, https://doi.org/https://doi.org/10.1002/qj.2411, 2015.

465 Ferranti, L., Magnusson, L., Vitart, F., and Richardson, D. S.: How far in advance can we predict changes in large-scale flow leading to severe cold conditions over Europe?, Quarterly Journal of the Royal Meteorological Society, 144, 1788–1802, https://doi.org/https://doi.org/10.1002/qj.3341, 2018.

Fetterer, F., Knowles, K., Meier, W. N., Savoie, M., and Windnagel, A. K.: Sea Ice Index, Version 3, https://doi.org/https://doi.org/10.7265/N5K072F8., accessed 2018, 2018.

470 Frame, T. H. A., Methven, J., Gray, S. L., and Ambaum, M. H. P.: Flow-dependent predictability of the North Atlantic jet, Geophys. Res. Lett., 40, 2411–2416, https://agupubs.onlinelibrary.wiley.com/doi/full/10.1002/grl.50454, 2013.

Frías, M. D., Herrera, S., Cofiño, A. S., and Gutiérrez, J. M.: Assessing the skill of precipitation and temperature seasonal forecasts in Spain: Windows of opportunity related to ENSO events, J. Climate, 23, 209–220, https://doi.org/https://doi.org/10.1175/2009JCLI2824.1, 2010.

Giorgetta, M. A., Jungclaus, J., Reick, C. H., Legutke, S., Bader, J., Böttinger, M., Brovkin, V., Crueger, T., Esch, M., Fieg, K., Glushak,
475 K., Gayler, V., Haak, H., Hollweg, H.-D., Ilyina, T., Kinne, S., Kornblueh, L., Matei, D., Mauritsen, T., Mikolajewicz, U., Mueller, W.,

Notz, D., Pithan, F., Raddatz, T., Rast, S., Redler, R., Roeckner, E., Schmidt, H., Schnur, R., Segschneider, J., Six, K. D., Stockhause, M., Timmreck, C., Wegner, J., Widmann, H., Wieners, K.-H., Claussen, M., Marotzke, J., and Stevens, B.: Climate and carbon cycle changes from 1850 to 2100 in MPI-ESM simulations for the Coupled Model Intercomparison Project phase 5, Journal of Advances in Modeling Earth Systems, 5, 572–597, https://doi.org/10.1002/jame.20038, 2013.

480   Goddard, L. and Dilley, M.: El Niño: Catastrophe or opportunity, J. Climate, 18, 651–665, https://doi.org/https://doi.org/10.1175/JCLI-3277.1, 2005.

Goeber, M., Wilson, C. A., Milton, S. F., and Stephenson, D. B.: Fairplay in the verification of operational quantitative precipitation forecasts, Journal of Hydrology, 288, 225–236, https://empslocal.ex.ac.uk/people/staff/dbs202/publications/2004/goeber.pdf, 2004.

Grönås, S.: Systematic errors and forecast quality of ECMWF forecasts in different large-scale flow patterns, in: Seminar on Interpretation
485   of Numerical Weather Prediction Products, 13-17 September 1982, pp. 161–206, ECMWF, ECMWF, Shinfield Park, Reading, https://www.ecmwf.int/node/9654, 1982.

Grönås, S.: A pilot study on the prediction of medium range forecast quality, ECMWF Technical Memoranda, p. 22, https://doi.org/10.21957/ostzejo17, 1985.

Hamill, T. M. and Juras, J.: Measuring forecast skill: is it real skill or is it the varying climatology?, Quarterly Journal of the Royal Meteo-
490   rological Society, 132, 2905–2923, https://doi.org/10.1256/qj.06.25, 2006.

Höschel, I., Illing, S., Grieger, J., Ulbrich, U., and Cubasch, U.: On skillful decadal predictions of the subpolar North Atlantic, Meteorologische Zeitschrift, 28, 417–428, https://doi.org/10.1127/metz/2019/0957, http://dx.doi.org/10.1127/metz/2019/0957, 2019.

Jones, C., Waliser, D. E., Lau, K. M., and Stern, W.: The Madden–Julian oscillation and its impact on northern hemisphere weather predictability, Mon. Wea. Rev., 132, 1462–1471, https://journals.ametsoc.org/view/journals/mwre/132/6/1520-0493_2004_132_1462_
495   tmoaii_2.0.co_2.xml, 2004.

Jones, C., Hazra, A., and Carvalho, L. M. V.: The Madden-Julian Oscillation and boreal winter forecast skill: An analysis of NCEP CFSv2 reforecasts, J. Climate, 28, 6297–6307, https://journals.ametsoc.org/view/journals/clim/28/15/jcli-d-15-0149.1.xml, 2015.

Kadow, C., Illing, S., Kunst, O., Rust, H. W., Pohlmann, H., Müller, W. A., and Cubasch, U.: Evaluation of forecasts by accuracy and spread in the MiKlip decadal climate prediction system, Meteorologische Zeitschrift, 25, 631–643, https://doi.org/10.1127/metz/2015/0639, 2016.

500   Kadow, C., Illing, S., Lucio-Eceiza, E., Bergemann, M., Ramadoss, M., Sommer, P., Kunst, O., Schartner, T., Pankatz, K., Grieger, J., Schuster, M., Richling, A., Thiemann, H., Kirchner, I., Rust, H., Ludwig, T., Cubasch, U., and Ulbrich, U.: Introduction to Freva – A Free Evaluation System Framework for Earth System Modeling, Journal of Open Research Software, 9, https://doi.org/10.5334/jors.253, 2021.

Kim, H.-M., Webster, P. J., and Curry, J. A.: Seasonal prediction skill of ECMWF System 4 and NCEP CFSv2 retrospective forecast for the Northern Hemisphere Winter, Climate Dyn., 39, 2957–2973, https://doi.org/https://doi.org/10.1007/s00382-012-1364-6, 2012.

505   Kröger, J., Pohlmann, H., Sienz, F., Marotzke, J., Baehr, J., Köhl, A., Modali, K., Polkova, I., Stammer, D., Vamborg, F. S. E., and Müller, W. A.: Full-field initialized decadal predictions with the MPI earth system model: an initial shock in the North Atlantic, Climate Dynamics, 51, 2593–2608, ISSN 1432-0894, https://doi.org/10.1007/s00382-017-4030-1, 2018.

Kruschke, T., Rust, H. W., Kadow, C., Müller, W. A., Pohlmann, H., Leckebusch, G. C., and Ulbrich, U.: Probabilistic evaluation of decadal prediction skill regarding Northern Hemisphere winter storms, Meteorologische Zeitschrift, 25, 721–738,
510   https://doi.org/10.1127/metz/2015/0641, 2016.

Manzanas, R., Frías, M. D., Cofiño, A. S., and Gutiérrez, J. M.: Validation of 40 year multimodel seasonal precipitation forecasts: The role of ENSO on the global skill, J. Geophys. Res. Atmos., 119, 1708–1719, https://doi.org/https://doi.org/10.1002/2013JD020680, 2014.

Mariotti, A., Baggett, C., Barnes, E. A., Becker, E., Butler, A., Collins, D. C., Dirmeyer, P. A., Ferranti, L., Johnson, N. C., Jones, J., Kirtman, B. P., Lang, A. L., Molod, A., Newman, M., Robertson, A. W., Schubert, S., Waliser, D. E., and Albers, J.: Windows of Opportunity for Skillful Forecasts Subseasonal to Seasonal and Beyond, Bulletin of the American Meteorological Society, 101, E608 – E625, https://doi.org/10.1175/BAMS-D-18-0326.1, 2020.

Marotzke, J., Müller, W. A., Vamborg, F. S. E., Becker, P., Cubasch, U., Feldmann, H., Kaspar, F., Kottmeier, C., Marini, C., Polkova, I., Prömmel, K., Rust, H. W., Stammer, D., Ulbrich, U., Kadow, C., Köhl, A., Kröger, J., Kruschke, T., Pinto, J. G., Pohlmann, H., Reyers, M., Schröder, M., Sienz, F., Timmreck, C., and Ziese, M.: MiKlip - a National Research Project on Decadal Climate Prediction, Bulletin of the American Meteorological Society, p. Early Online Releases, https://doi.org/10.1175/BAMS-D-15-00184.1, 2016.

Mauritsen, T., Bader, J., Becker, T., Behrens, J., Bittner, M., Brokopf, R., Brovkin, V., Claussen, M., Crueger, T., Esch, M., Fast, I., Fiedler, S., Fläschner, D., Gayler, V., Giorgetta, M., Goll, D. S., Haak, H., Hagemann, S., Hedemann, C., Hohenegger, C., Ilyina, T., Jahns, T., Jimenéz-de-la Cuesta, D., Jungclaus, J., Kleinen, T., Kloster, S., Kracher, D., Kinne, S., Kleberg, D., Lasslop, G., Kornblueh, L., Marotzke, J., Matei, D., Meraner, K., Mikolajewicz, U., Modali, K., Möbis, B., Müller, W. A., Nabel, J. E. M. S., Nam, C. C. W., Notz, D., Nyawira, S.-S., Paulsen, H., Peters, K., Pincus, R., Pohlmann, H., Pongratz, J., Popp, M., Raddatz, T. J., Rast, S., Redler, R., Reick, C. H., Rohrschneider, T., Schemann, V., Schmidt, H., Schnur, R., Schulzweida, U., Six, K. D., Stein, L., Stemmler, I., Stevens, B., von Storch, J.-S., Tian, F., Voigt, A., Vrese, P., Wieners, K.-H., Wilkenskjeld, S., Winkler, A., and Roeckner, E.: Developments in the MPI-M Earth System Model version 1.2 (MPI-ESM1.2) and Its Response to Increasing CO2, Journal of Advances in Modeling Earth Systems, 11, 998–1038, https://doi.org/10.1029/2018MS001400, 2019.

Miller, D. E. and Wang, Z.: Assessing seasonal predictability sources and windows of high predictability in the climate forecast system, version 2, J. Climate, 32, 1307–1326, https://doi.org/https://doi.org/10.1175/JCLI-D-18-0389.1, 2019.

Morice, C. P., Kennedy, J. J., Rayner, N. A., and Jones, P. D.: Quantifying uncertainties in global and regional temperature change using an ensemble of observational estimates: The HadCRUT4 data set, Journal of Geophysical Research: Atmospheres, 117, https://doi.org/https://doi.org/10.1029/2011JD017187, https://agupubs.onlinelibrary.wiley.com/doi/abs/10.1029/2011JD017187, 2012.

Murphy, A. H.: General Decompositions of MSE-Based Skill Scores: Measures of Some Basic Aspects of Forecast Quality, Monthly Weather Review, 124, 2353–2369, https://doi.org/10.1175/1520-0493(1996)124<2353:GDOMBS>2.0.CO;2, 1996.

Müller, W. A., Pohlmann, H., Sienz, F., and Smith, D.: Decadal climate predictions for the period 1901-2010 with a coupled climate model, Geophys. Res. Lett., 41, 2100–2107, https://doi.org/https://doi.org/10.1002/2014GL059259, 2014.

Müller, W. A., Jungclaus, J. H., Mauritsen, T., Baehr, J., Bittner, M., Budich, R., Bunzel, F., Esch, M., Ghosh, R., Haak, H., Ilyina, T., Kleine, T., Kornblueh, L., Li, H., Modali, K., Notz, D., Pohlmann, H., Roeckner, E., Stemmler, I., Tian, F., and Marotzke, J.: A Higher-resolution Version of the Max Planck Institute Earth System Model (MPI-ESM1.2-HR), Journal of Advances in Modeling Earth Systems, 10, 1383–1413, https://doi.org/10.1029/2017MS001217, 2018.

Pasternack, A., Bhend, J., Liniger, M. A., Rust, H. W., Müller, W. A., and Ulbrich, U.: Parametric decadal climate forecast recalibration (DeFoReSt 1.0), Geoscientific Model Development, 11, 351–368, https://doi.org/10.5194/gmd-11-351-2018, 2018.

Pasternack, A., Grieger, J., Rust, H. W., and Ulbrich, U.: Recalibrating decadal climate predictions – what is an adequate model for the drift?, Geoscientific Model Development, 14, 4335–4355, https://doi.org/10.5194/gmd-14-4335-2021, 2021.

Pearson, K., Lee, A., and Bramley-Moore, L.: VI. Mathematical contributions to the theory of evolution. —VI. Genetic (reproductive) selection: Inheritance of fertility in man, and of fecundity in thoroughbred racehorses, Philosophical Transactions of the Royal Society of London. Series A, Containing Papers of a Mathematical or Physical Character, 192, 257–330, https://doi.org/10.1098/rsta.1899.0006, 1899.

Peter, M., Rust, H. W., and Ulbrich, U.: Interannual variations in the seasonal cycle of extreme precipitation in Germany and the response to climate change, Natural Hazards and Earth System Sciences, 24, 1261–1285, https://doi.org/10.5194/nhess-24-1261-2024, https://nhess.copernicus.org/articles/24/1261/2024/, 2024.

Pohlmann, H., Müller, W. A., Kulkarni, K., Kameswarrao, M., Matei, D., Vamborg, F. S. E., Kadow, C., Illing, S., and Marotzke, J.: Improved forecast skill in the tropics in the new MiKlip decadal climate predictions, Geophysical Research Letters, 40, 5798–5802, https://doi.org/10.1002/2013GL058051, 2013.

Pohlmann, H., Müller, W. A., Bittner, M., Hettrich, S., Modali, K., Pankatz, K., and Marotzke, J.: Realistic Quasi-Biennial Oscillation Variability in Historical and Decadal Hindcast Simulations Using CMIP6 Forcing, Geophysical Research Letters, 46, 14 118–14 125, https://doi.org/10.1029/2019GL084878, 2019.

Polkova, I., Brune, S., Kadow, C., Romanova, V., Gollan, G., Baehr, J., Glowienka-Hense, R., Greatbatch, R. J., Hense, A., Illing, S., Köhl, A., Kröger, J., Müller, W. A., Pankatz, K., and Stammer, D.: Initialization and Ensemble Generation for Decadal Climate Predictions: A Comparison of Different Methods, Journal of Advances in Modeling Earth Systems, 11, 149–172, https://doi.org/https://doi.org/10.1029/2018MS001439, 2019.

Qin, J. and Robinson, W. A.: The impact of tropical forcing on extratropical predictability in a simple global model, J. Atmos. Sci., 52, 3895–3910, https://doi.org/https://doi.org/10.1175/1520-0469(1995)052<3895:TIOTFO>2.0.CO;2, 1995.

Richardson, D., Black, A. S., Monselesan, D. P., II, T. S. M., Risbey, J. S., Schepen, A., Squire, D. T., and Tozer, C. R.: Identifying Periods of Forecast Model Confidence for Improved Subseasonal Prediction of Precipitation, Journal of Hydrometeorology, 22, 371 – 385, https://doi.org/10.1175/JHM-D-20-0054.1, 2021.

Simpson, E. H.: The Interpretation of Interaction in Contingency Tables, Journal of the Royal Statistical Society: Series B (Methodological), 13, 238–241, https://doi.org/10.1111/j.2517-6161.1951.tb00088.x, 1951.

Tibaldi, S. and Molteni, F.: On the operational predictability of blocking, Tellus, 42A, 343–365, https://doi.org/10.1034/j.1600-0870.1990.t01-2-00003.x, - 1D blocking index, based on Okland blocking index - but additional criteria (e.g. duration, zonal flow gradients) - most common used blocking index - frequency of blocking depends on forecast time - climatology, 1990.

Uppala, S. M., KÅllberg, P. W., Simmons, A. J., Andrae, U., Bechtold, V. D. C., Fiorino, M., Gibson, J. K., Haseler, J., Hernandez, A., Kelly, G. A., Li, X., Onogi, K., Saarinen, S., Sokka, N., Allan, R. P., Andersson, E., Arpe, K., Balmaseda, M. A., Beljaars, A. C. M., Berg, L. V. D., Bidlot, J., Bormann, N., Caires, S., Chevallier, F., Dethof, A., Dragosavac, M., Fisher, M., Fuentes, M., Hagemann, S., Hólm, E., Hoskins, B. J., Isaksen, L., Janssen, P. A. E. M., Jenne, R., Mcnally, A. P., Mahfouf, J.-F., Morcrette, J.-J., Rayner, N. A., Saunders, R. W., Simon, P., Sterl, A., Trenberth, K. E., Untch, A., Vasiljevic, D., Viterbo, P., and Woollen, J.: The ERA-40 re-analysis, Quarterly Journal of the Royal Meteorological Society, 131, 2961–3012, ISSN 1477-870X, https://doi.org/10.1256/qj.04.176, 2005.

Wilks, D. S.: Statistical Methods in the Atmospheric Sciences, Academic Press, San Diego, CA, 3rd edn., 2011.

Yule, G. U.: Notes on the theory of association of attributes in statistics, Biometrika, 2, 121–134, ISSN 0006-3444, https://doi.org/10.1093/biomet/2.2.121, 1903.

Zhang, J. and Zhang, R.: On the evolution of Atlantic Meridional Overturning Circulation fingerprint and implications for decadal predictability in the North Atlantic, Geophys. Res. Lett., 42, 5419–5426, https://doi.org/https://doi.org/10.1002/2015GL064596, 2015.